Synchrotron-based measurement of the impact of thermal cycling on the evolution of stresses in Cu through-silicon vias

Chukwudi Okoro, Lyle E. Levine, Ruqing Xu, Klaus Hummler, and Yaw Obeng

Citation: Journal of Applied Physics **115**, 243509 (2014); doi: 10.1063/1.4885461
View online: http://dx.doi.org/10.1063/1.4885461
View Table of Contents: http://scitation.aip.org/content/aip/journal/jap/115/24?ver=pdfcov
Published by the AIP Publishing

Synchrotron-based measurement of the impact of thermal cycling on the evolution of stresses in Cu through-silicon vias

Chukwudi Okoro,[1,a)] Lyle E. Levine,[2] Ruqing Xu,[3] Klaus Hummler,[4] and Yaw Obeng[1]
[1]*Semiconductor and Dimensional Metrology Division, National Institute of Standards and Technology (NIST), Gaithersburg, Maryland 20899, USA*
[2]*Material Science and Engineering Division, National Institute of Standards and Technology (NIST), Gaithersburg, Maryland 20899, USA*
[3]*Advanced Photon Source, Argonne National Laboratory, Argonne, Illinois 60439-4800, USA*
[4]*SEMATECH, 257 Fuller Road, Albany, New York 12203, USA*

(Received 14 May 2014; accepted 15 June 2014; published online 30 June 2014)

One of the main causes of failure during the lifetime of microelectronics devices is their exposure to fluctuating temperatures. In this work, synchrotron-based X-ray micro-diffraction is used to study the evolution of stresses in copper through-silicon via (TSV) interconnects, "as-received" and after 1000 thermal cycles. For both test conditions, significant fluctuations in the measured normal and shear stresses with depth are attributed to variations in the Cu grain orientation. Nevertheless, the mean hydrostatic stresses in the "as-received" Cu TSV were very low, at (16 ± 44) MPa, most likely due to room temperature stress relaxation. In contrast, the mean hydrostatic stresses along the entire length of the Cu TSV that had undergone 1000 thermal cycles (123 ± 37) MPa were found to be eight times greater, which was attributed to increased strain-hardening. The evolution in stresses with thermal cycling is a clear indication that the impact of Cu TSVs on front-end-of-line (FEOL) device performance will change through the lifetime of the 3D stacked dies, and ought to be accounted for during FEOL keep-out-zone design rules development. © *2014 AIP Publishing LLC*.
[http://dx.doi.org/10.1063/1.4885461]

INTRODUCTION

Electronic devices are commonly subjected to temperature fluctuations during their operational lifetime. This incessant thermal cycling leads to thermal fatigue and subsequent failure of these devices.[1] Thermal fatigue results from the formation and growth of defects, such as cracks and voids, which arise from the continuous generation of reversal stresses caused by cyclic temperature loading. These stresses originate from the mismatch in the thermo-mechanical properties of the multi-materials of construction.

With the emergence of three-dimensional stacked integrated circuits (3D-SIC), as the microchip of the future, the concern for stress-related failures due to thermal fatigue has increased. This is because the vertical electrical connections through the stacked chips are achieved with copper interconnects, called through-silicon via (TSV), which are fabricated through the active silicon. Unfortunately, the large mismatch in the coefficients of thermal expansion (CTE) of copper ($17 \times 10^{-6}/°C$) and silicon ($2.3 \times 10^{-6}/°C$) leads to the generation of significant stresses.[2]

In order to understand and minimize thermal fatigue concerns in Cu TSV interconnects, a number of published studies have assessed the impact of thermal cycling on their reliability performance.[3–8] These studies focused on understanding how thermal cycling affected the electrical and electromagnetic characteristics of Cu TSVs, as well as its impact on damage formation and propagation. However, no published study has experimentally related the underlying root cause of the changes in the Cu TSV, i.e., the buildup of stresses, with the extent of thermal cycling. Since stress generation is the root cause of thermal fatigue, accurate stress characterization in Cu TSV interconnects is fundamental for the reduction of failures in 3D-SICs chips.

In previous reports, we developed and demonstrated a measurement procedure for the *in-situ* determination of the depth-dependent full strain/stress tensor in Cu TSVs using synchrotron-based X-ray micro-diffraction,[9–11] which requires no additional sample preparation that may alter the measurand.[12–14] In this study, we leverage this technique to investigate the effect of thermal cycling on the evolution of stresses in Cu TSVs.

EXPERIMENT

Sample

For this study, SEMATECH[15] built two-level stacked dies were used, and the details of fabrication are reported elsewhere.[16] The top die contained a daisy chain of 60 TSVs, with a pitch of 16 μm. Each TSV has a diameter and depth of about 5 μm and 50 μm, respectively. The details of the thermal history of the samples prior to their use for this experiment are presented in Table I.

The samples were stored at room temperature (RT) for more than nine months before being used for this experiment. For this work, two dies from the same Cu TSV wafer were studied; one sample only underwent fabrication-related thermal treatment (see Table I), and is called the "as-received" sample. The other sample, in addition to fabrication related heat treatment, was subjected to 1000 thermal

a)Email: chukwudi.okoro@nist.gov. Phone: 301-975-2040

TABLE I. Thermal history of the Cu TSV samples during their fabrication process prior to their usage for this experiment. This represents the "as-received" state of the samples.

Processing steps	Annealing temperature (°C)	Annealing time (min)
After Cu electro-plating	150	60
Front-side dielectric deposition	350	2
Back-side dielectric deposition	350	2
Etch stop deposition	400	2
After front-side metallization deposition	150	60
After back-side metallization deposition	150	60

cycles. Each thermal cycle involved reversal heating and cooling between minimum and maximum temperatures of 30 °C and 150 °C, respectively. A cycle was completed in about 6 min, and only one Cu TSV was measured for each test condition. Fig. 1 is an illustrative cross-sectional image of the stacked die used in this study; it is meant to show the details of the structure and the geometry of the stacked dies. The x-ray measurements were performed on only the top die that contained the TSVs.

X-ray micro-diffraction experiment

These synchrotron-based experiments were performed using the X-ray micro-diffraction instrument on sector 34-ID E at the Advanced Photon Source (APS), Argonne National

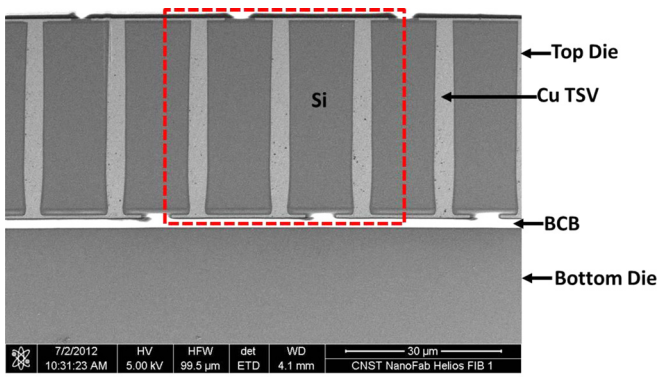

(a)

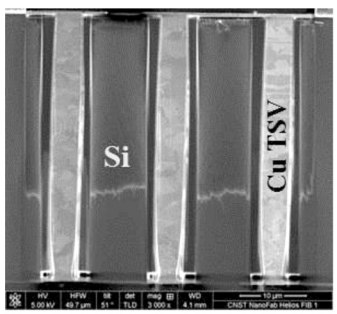

(b)

FIG. 1. Cross-sectional image of the stacked die used in this study (a) shows the entire cross-section of the stacked die. (b) is the SEM image of the boxed region in (a), after FIB milling. By milling using the FIB technique, the grain sizes of the Cu TSV microstructure were revealed.

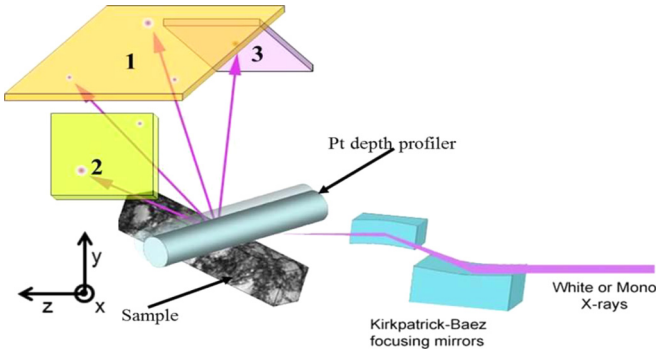

FIG. 2. Schematic diagram of the X-ray microbeam diffraction setup that was used for this experiment. Detector 1 is normal to the vertical direction, while detectors 2 and 3 are inclined at 45° with respect to detector 1.

Laboratory. In this work, three area detectors surrounded the intersection of the horizontal X-ray beam with the sample (see Fig. 2). The central detector (detector 1) was perpendicular to the vertical direction, while the other two detectors (detector 2 and detector 3) were inclined at 45°, each at the opposite sides of the central detector, thus maximizing the angular range of the detected diffracted beams. This arrangement minimizes measurement uncertainties for the extracted full strain and stress tensors from the Cu TSV. Depth resolution along the beam direction was made possible by the use of a platinum wire based depth profiler. A total of 11 measurements were performed along the length of the Cu TSV, at a translation step interval of 5 μm. The beam size was about 0.5 μm by 0.5 μm, with a depth resolution of about 1 μm. Both monochromatic and polychromatic X-rays were used to scan the Cu TSV.

From these X-ray micro-diffraction experiments, we obtain depth and detector dependent data, such as the matching reflection indices, coordinates of diffraction peaks on the detectors, and their uncertainties. These allow determination of local lattice parameters, crystallographic orientation, and uncertainties. Fig. 3 shows the energy-integrated diffraction peaks of the matching reflections and peak intensities (marked "**X**") from the three different detectors at a depth of 12.5 μm for the "as-received" Cu TSV. This information was used, in conjunction with the elastic constants and unstrained lattice parameter for Cu, to obtain the depth-dependent, full strain/stress tensors in the Cu TSV and the orientations of their grains.

Even though 11 measurements were performed along the Cu TSV for the two test conditions, only 7 and 10 measurements were reported for the "as-received" and the 1000 cycled samples, respectively. This is because the matching Laue reflections on the three different area detectors from the same sample volume at each unreported depth could not be unambiguously determined.

The full stress tensor results were initially computed in the coordinate system of the given crystal, then converted to the laboratory coordinate system using the reported Euler angles (φ, θ, ψ), and finally transformed to a coordinate system tied to the sample geometry. This was achieved by performing a 45° rotation about the X-axis, since the sample was inclined at 45° to the incident X-ray beam direction.

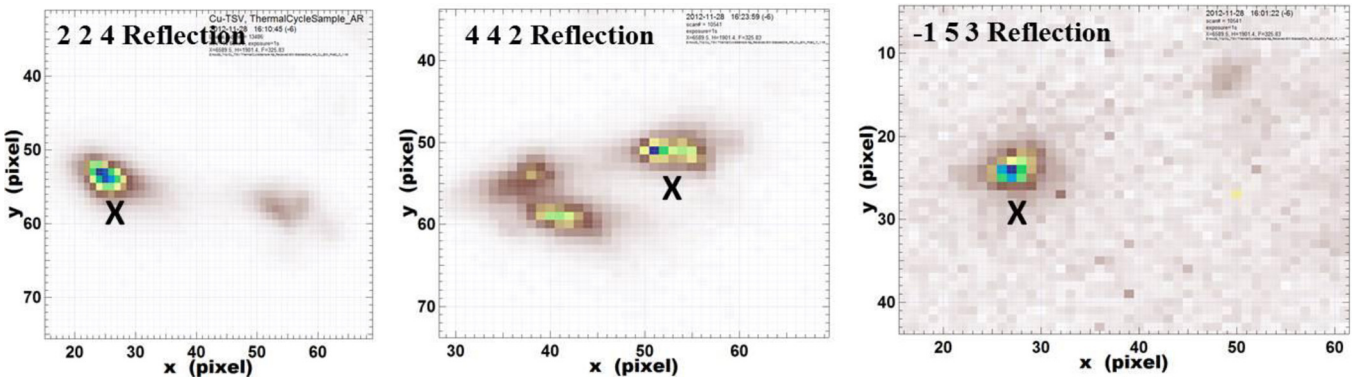

FIG. 3. Peaks of the matching Laue pattern reflections on the three different area detectors obtained after an energy scan using a monochromatic X-ray beam, for the "as-received" Cu TSV at a depth of ≈12.5 μm. (a) Detector 1, (b) detector 2, and (c) detector 3. The peaks marked "X" are the matching peaks from the different area detector reflections.

This leads to the determination of the full stress tensor (σ) in the Cu TSVs which is represented in a matrix form in the following equation:

$$\sigma = \begin{pmatrix} \sigma_{11} & \sigma_{12} & \sigma_{13} \\ \sigma_{21} & \sigma_{22} & \sigma_{23} \\ \sigma_{31} & \sigma_{32} & \sigma_{33} \end{pmatrix}. \quad (1)$$

The stress components, σ_{11}, σ_{22}, and σ_{33} are the normal stresses, where, σ_{11} and σ_{22} are the in-plane normal stresses and σ_{33} the out-of-plane normal stress. The other stress components in the matrix are the shear stresses. Due to symmetry, the stress tensor is reduced to only six stress components, since, $\sigma_{12} = \sigma_{21}$, $\sigma_{13} = \sigma_{31}$, $\sigma_{23} = \sigma_{32}$.

It is worth noting that the depth along the Cu TSV of each measurement is only known within a 5 μm window, as the selected grain could be anywhere along the intersection of the incident X-ray beam with the selected Cu TSV. Thus, the mean depth is used for all reported measurement results. For instance, the measurement done between 5 μm and 10 μm is assumed to be measured at a depth of 7.5 μm.

A detailed description of the measurement procedure used in this study was reported elsewhere in Refs. [12–14].

RESULTS

Normal stresses

Fig. 4 shows the depth-dependent normal stresses in the "as-received" sample. The uncertainties overlap at each depth, demonstrating the normal stress state is largely hydrostatic. Note that the hydrostatic stress is defined as the average of the σ_{11}, σ_{22}, and σ_{33}. While the top region of the Cu TSV was in compression, with an average value of (-33 ± 44) MPa, a maximum hydrostatic stress of (38 ± 91) MPa was measured at the bottom of the Cu TSV. The normal stresses fluctuated along the entire Cu TSV depth, with a mean absolute value of (16 ± 44) MPa.

Fig. 5 presents the measured normal stresses for the 1000 thermal cycled Cu TSV sample, which were found to continuously fluctuate along the depth of the Cu TSV. With the exception of depths from 12.5 μm to 27.5 μm, the normal stresses in the cycled sample were largely hydrostatic, just as the "as-received" sample. The minimum hydrostatic stresses of (30 ± 27) MPa (top) and (18 ± 35) MPa (bottom) were found to occur at the ends of the Cu TSV, while the maximum normal stresses of (353 ± 21) MPa were measured at

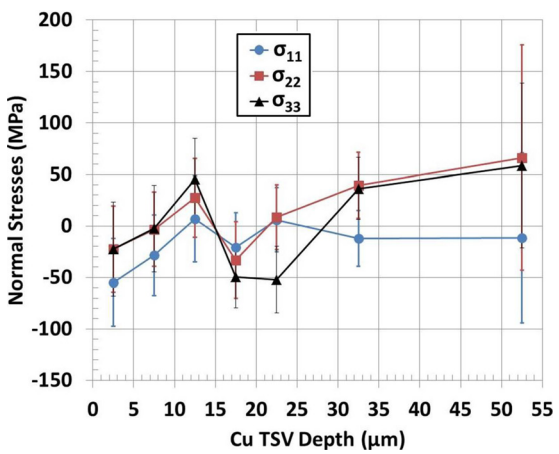

FIG. 4. The experimentally determined normal stresses for the "as-received" Cu TSV sample with respect to depth. The one standard deviation uncertainties result from uncertainties in the diffracted X-ray peak positions on the area detectors and uncertainties in the lattice spacing determination.

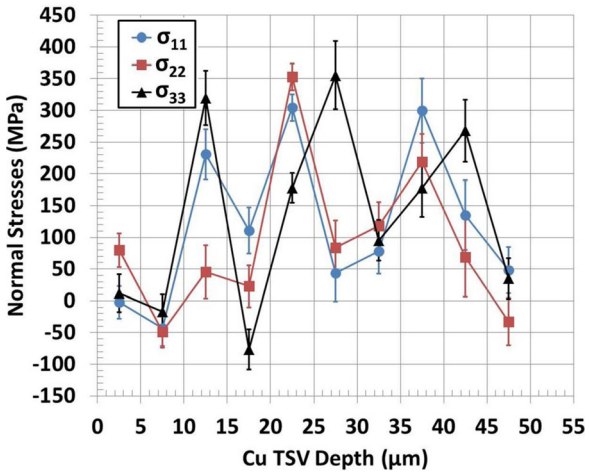

FIG. 5. The experimentally determined normal stresses for the 1000 thermally cycled Cu TSV sample with respect to depth. The one standard deviation uncertainties result from uncertainties in the diffracted X-ray peak positions on the area detectors and uncertainties in the lattice spacing determination.

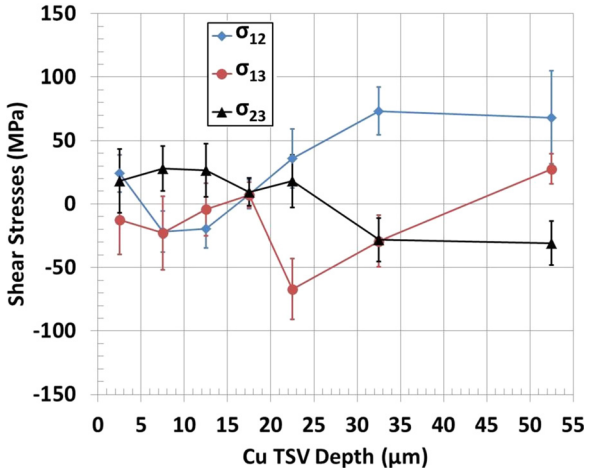

FIG. 6. The experimentally determined shear stresses for the "as-received" Cu TSV sample with respect to depth. The one standard deviation uncertainties result from uncertainties in the diffracted X-ray peak positions on the area detectors and uncertainties in the lattice spacing determination.

the center of the Cu TSV. Thus, the normal stresses show an approximately "bow-like" profile. The mean hydrostatic stress, obtained by averaging the hydrostatic stresses from all the depths, was (123 ± 37) MPa.

Shear stresses

The measured shear stresses (σ_{12}, σ_{13}, and σ_{23}) of the "as-received" sample are presented in Fig. 6. Their values were approximately constant and overlapping at the top region ($\leq$17.5 μm) of the Cu TSV, with mean absolute shear stress value of ≈20 MPa. However, for depths $\geq$22.5 μm, a large fluctuation and discrepancy in the values of the different shear stresses was measured, with values much higher than that measured at the top region of the Cu TSV. For instance, a maximum shear stress value of (73 ± 19) MPa was measured at the depth of 32.5 μm. The mean absolute shear stress along the entire length of the "as-received" sample is (28 ± 20) MPa.

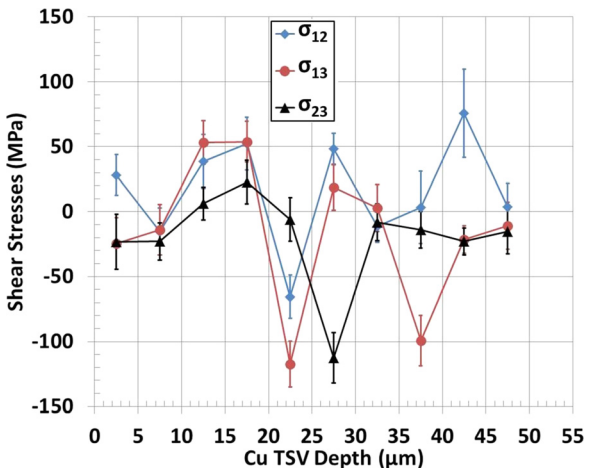

FIG. 7. The experimentally determined normal stresses for the 1000 thermally cycled Cu TSV sample with respect to its depth. The one standard deviation uncertainties result from uncertainties in the diffracted X-ray peak positions on the area detectors and uncertainties in the lattice spacing determination.

The measured shear stresses in the 1000 cycled Cu TSV sample are presented in Fig. 7. The values of the three different shear stresses overlap at the top region ($\leq$17.5 μm) of the Cu TSV, similar to the "as-received" sample (Fig. 6). However, the values of the shear stresses in the 1000 cycled sample are much larger than the "as-received," especially at the central region of the Cu TSV, where the maximum shear stress of (−118 ± 18) MPa was measured at 22.5 μm depth. The mean absolute shear stress along the entire length of the 1000 cycled sample is ≈34 MPa.

Grain orientation

As discussed previously, the crystallographic orientation of each grain was determined, allowing us to calculate the crystallographic axis that is parallel to the TSV axis. Since these axes are typically low symmetry directions, Table II shows the nearest high symmetry axis for all measured depths in both Cu TSV samples. For both test conditions, the orientations of the grains were found to be dissimilar across the depth of the TSV with the exception of the 2.5 μm and 7.5 μm depths for the "as-received" Cu TSV. The diffraction data from these two depths came from distinct dislocation cell interiors at widely separated locations within a single grain that was much greater than 5 μm across.

DISCUSSION

The significant fluctuations in the measured stresses (Figs. 4–7) with Cu TSV depth, for both the "as-received" and the 1000 cycled samples are attributed to the anisotropy of the Cu, as confirmed by Table II. In this table, the grain orientations for both test conditions were found to vary with depth, with the exception of the top region ($\leq$7.5 μm) of the "as-received" sample. Since numerous material properties of metals are dependent on grain orientation, they are expected to significantly influence the measured stress values.

From Figs. 4 and 5, it was observed that independent of the thermal cycling condition, for majority of the depths, the normal stresses were roughly equal, indicating that the Cu TSVs were largely in a hydrostatic stress state. Additionally, the minimum normal stresses were observed to occur at the

TABLE II. Nearest high-symmetry crystallographic orientations along the Cu TSV axis of grain in the "as-received" and the 1000 cycled Cu TSVs with respect to depth.

Depth (μm)	As-received Cu TSV	1000 cycled Cu TSV
2.5	$(\bar{1}3\bar{1})$	$(\bar{2}12)$
7.5	$(\bar{1}3\bar{1})$	$(\bar{1}\bar{1}4)$
12.5	$(\bar{1}30)$	$(\bar{2}11)$
17.5	$(\bar{4}\bar{2}1)$	$(\bar{2}\bar{1}\bar{2})$
22.5	$(\bar{3}\bar{1}0)$	(031)
27.5	…	$(\bar{2}02)$
32.5	(101)	(114)
37.5	…	$(1\bar{1}\bar{2})$
42.5	…	$(\bar{1}1\bar{2})$
47.5	…	$(12\bar{2})$
52.5	$(03\bar{1})$	…

top region of the Cu TSV. For the 1000 cycled sample (Fig. 5), the minimum normal stresses occur at both ends of the Cu TSV, with the maximum normal stresses occurring at the center of the Cu TSV, thus displaying an approximately "bow-like" stress profile. This stress profile is related to the varying constraint on the Cu TSV, where the ends which have less constraint witness lower stresses, and the Cu TSV center, being the most constrained region, witnesses the highest stresses. This approximately "bow-like" profile of the normal stresses is in agreement with FEM studies reported elsewhere.[4]

The measured normal and shear stresses in the "as-received" Cu TSV (Figs. 4 and 6) were found to be very low, with a mean hydrostatic stress and absolute shear stress of (16 ± 44) MPa and (28 ± 20) MPa, respectively, along the entire Cu TSV. These values are very low in comparison with all reported studies on Cu TSV stresses.[12,13,17,18] The low stress values may be attributed to stress relaxation in the "as-received" sample. Since the sample was measured more than nine months after its fabrication, the stresses in the Cu TSV are expected to decrease due to RT stress relaxation.[19–24] RT stress relaxation may occur due to rate-controlled mechanisms, such as self-annealing (also called RT recrystallization) or the motion of dislocations. The former mechanism is governed by the nucleation and the growth of grains,[22–24] while the latter mechanism is governed by the motion of dislocation.[19–21] Here, RT stress relaxation is attributed to dislocation motion. This is because, during the fabrication process, the Cu TSV samples underwent thermal treatment involving temperatures up to 400 °C (see Table I), which is sufficient for achieving full grain growth and microstructural stability of Cu interconnects. This temperature is also the maximum temperature that the microelectronic chip will ever undergo during its lifetime.[24–27] On the other hand, RT stress relaxation governed by self-annealing occurs in electroplated Cu when the structures receive minimal post-electroplating heat treatment.

In contrast, the normal stresses for the 1000 cycled sample (Fig. 5) were found to be much greater, with a maximum hydrostatic stress of (353 ± 21) MPa in the central region and an average hydrostatic stress of (123 ± 37) MPa along the entire length of the Cu TSV. This means that stresses in the 1000 cycled Cu TSV are approximately eight times greater than those in the "as-received" Cu TSV (Fig. 4). This stress increase after 1000 thermal cycles was attributed to strain hardening. As depicted schematically in Fig. 8, it is expected that thermal cycling will initially lead to an increase in stress in the Cu TSV due to the increase in dislocation density and their entanglement, leading to strain hardening. However, after a critical stress level is reached, continued thermal cycling will lead to the significant growth and the coalescing of defects, such as micro-cracks or micro-voids.[28–32] Such defects are known to promote stress relief in metals, when they attain a critical size. This drop in the residual stresses is expected to become more pronounced as the cracks and voids in the structure increase with thermal cycling. This suggests that there are two competing mechanisms that influence the evolution of stresses with thermal cycling; strain-hardening and damage.

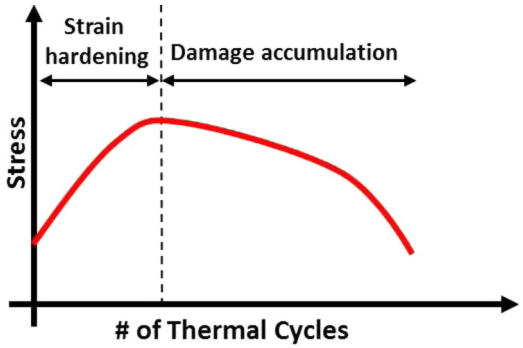

FIG. 8. Schematic graph showing the change in stress with the number of thermal cycles.

This proposition is further supported by measurements from our prior study, in which we performed failure analyses to determine the impact of thermal cycling on crack and void growth on dies from the same wafer as those used in this present study.[4] Fig. 9 illustrates the effect of thermal cycling on sidewall crack growth at the Cu - isolation liner interface of the TSV.

The data clearly show that the measured crack length at the Cu TSV sidewall remains statistically unchanged even after 1000 thermal cycles, however, the spread in the data increases after 2000 cycles. This is in agreement with our proposition that the measured increase in the stresses in the Cu TSVs after 1000 cycles is due to strain hardening, as no substantial growth in cracks was measured.

The measured change in the Cu TSV stresses with thermal cycling is anticipated to have an impact on the in-service performance of neighboring front-end-of-line (FEOL) devices, such as transistors.[33–35] This is because 3D stacked dies will be subjected to continuously fluctuating cyclic temperatures during their lifetime, leading to large changes in the Cu TSV stresses. This, in turn, will lead to changes in the performance of integrated FEOLs over their lifetime. While today's keep-out zone (KOZ) design rules are based on the static stresses in the TSV, mainly in the "as-received" state, it may be necessary to account for stress evolution in Cu TSVs over their projected lifetime.

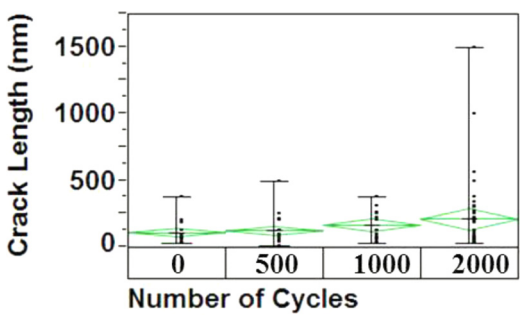

FIG. 9. Effect of thermal cycling on the sidewall crack length at the Cu–barrier interface. It is a reprinted with permission from C. Okoro, F. Golshany, J. W. Lau, K. Hummler, and Y. S. Obeng, "A detailed failure analysis examination of the effect of thermal cycling on Cu TSV reliability," IEEE Trans. Electron Devices **61**(1), 15–22 (2014). Copyright 2014 IEEE Electron Devices Society. The error bars represent ± three times the standard deviation (sigma) of the arithmetic mean of the measurements. The data variability is a composite of sample-to-sample variability and systematic experimental variability.

Future studies are planned to identify the critical number of cycles at which stress evolution transitions from being strain-hardening controlled to being damage accumulation controlled.

CONCLUSION

In this study, synchrotron X-ray micro-diffraction measurements were used to study the impact of thermal cycling on the stress evolution in Cu TSVs. The full stress tensor in Cu TSVs was determined with respect to position along the Cu TSV. Two test conditions were studied: "as-received" (no thermal cycling) and 1000 cycled Cu TSVs.

The significant fluctuation of stresses along the Cu TSV for both the "as-received" and the 1000 cycled samples was attributed to the microstructural variations, notably the grain orientation.

The minimum normal stresses occurred at the ends of the Cu TSV, due to the limited constraint in this region. For the 1000 cycled sample, the profile of the normal stresses was found to be approximately "bow-like."

The stresses in the "as-received" sample were low, with a mean absolute hydrostatic stress value of (16 ± 44) MPa. The low stress values were attributed to stress relaxation due to dislocation motion, resulting from their RT storage for nine months. The mean hydrostatic stresses along the entire Cu TSV in the 1000 cycled sample were found to be about eight times greater than those in the "as-received" sample. The increase in stress with thermal cycling is attributed to strain-hardening, which is caused by the increased dislocation density and dislocation entanglement.

Since the stresses in the surrounding silicon are induced by Cu TSV stresses, it is anticipated that the evolution of Cu TSV stresses with thermal cycling will lead to performance changes of surrounding FEOL devices over their lifetime. Thus, it is essential that implemented KOZ design rules should take into account the evolution of stresses in Cu TSVs over their projected lifetime.

ACKNOWLEDGMENTS

The XOR/UNI facilities on Sector 34 at the APS are supported by the U.S. Department of Energy (DOE), Office of Science, Office of Basic Energy Sciences, under Contract No. DE-AC02-06CH11357.

[1]M. Pei, R. Han, D. Kwon, A. Lucero, V. Vasudevan, R. Kwasnick, and P. S. Polasam, "Define electrical packing temperature cycling requirement with field measured user behavior data," in *63rd Proceedings of the Electronics Components and Technology Conference (ECTC), Las Vegas, NV, May 2013* (IEEE, 2013), pp. 159–165.
[2]L. W. Kong, J. R. Lloyd, K. B. Yeap, E. Zschech, A. Rudack, M. Liehr, and A. Diebold, "Applying X-ray microscopy and finite element modeling to identify the mechanism of stress-assisted void growth in through-silicon vias," J. Appl. Phys. **110**(5), 053502 (2011).
[3]C. Okoro, P. Kabos, J. Obrzut, K. Hummler, and Y. S. Obeng, "Accelerated stress test assessment of through-silicon via using RF signals," IEEE Trans. Electron Devices **60**(6), 2015–2021 (2013).
[4]C. Okoro, F. Golshany, J. W. Lau, K. Hummler, and Y. S. Obeng, "A detailed failure analysis examination of the effect of thermal cycling on Cu TSV reliability," IEEE Trans. Electron Devices **61**(1), 15–22 (2014).
[5]M. G. Farooq *et al.*, "3D copper TSV integration, testing and reliability," in *International Electron Devices Meeting (IEDM), Washington, DC, Dec. 2011* (IEEE, 2011), pp. 7.1.1–7.1.4.
[6]X. Liu, Q. Chen, V. Sundaram, R. R. Tummala, and S. K. Sitaraman, "Failure analysis of through-silicon vias in free-standing wafer under thermal-shock test," Microelectron. Reliab. **53**, 70–78 (2013).
[7]T. Frank *et al.*, "Reliability approach of high density through silicon via (TSV)," in *60th Proceedings of the Electronics Components and Technology Conference (ECTC), Las Vegas, NV, June 2010* (IEEE, 2010), pp. 321–324.
[8]P. Kumar, I. Dutta, and M. S. Bakir, "Interfacial effects during thermal cycling of Cu-filled through-silicon vias (TSV)," J. Electron. Mater. **41**, 322–335 (2012).
[9]B. C. Larson and L. E. Levine, "Submicrometer-resolution polychromatic 3D X-ray microscopy," J. Appl. Cryst. **46**, 153–164 (2013).
[10]L. E. Levine, P. Geantil, B. C. Larson, J. Z. Tischler, M. E. Kassner, W. Liu, M. R. Stoudt, and F. Tavazza, "Disordered long range internal stresses in deformed copper and the mechanisms underlying plastic deformation," Acta Mater. **59**, 5803–5811 (2011).
[11]L. E. Levine, B. C. Larson, W. Yang, M. E. Kassner, J. Z. Tischler, M. A. Delos-Reyes, R. J. Fields, and W. Liu, "X-ray microbeam measurements of individual dislocation cell elastic strains in deformed single crystal copper," Nature Mater. **5**, 619–622 (2006).
[12]C. Okoro, L. E. Levine, J. Z. Tischler, R. Xu, W. Liu, O. Kirillov, K. Hummler, and Y. S. Obeng, "X-ray micro-beam diffraction determination of full stress tensors in Cu TSVs," in *63th Proceedings of the Electronics Components and Technology Conference (ECTC), Las Vegas, NV, May 2013* (IEEE, 2013), pp. 648–652.
[13]C. Okoro, L. E. Levine, R. Xu, K. Hummler, and Y. Obeng, "Non-destructive measurement of the residual stresses in copper through-silicon vias using synchrotron-based micro-beam X-ray diffraction," IEEE Trans. Electron Devices **61**, 2473–2479 (2014).ôôôô
[14]L. E. Levine, C. Okoro, and R. Xu, "Full elastic strain tensor measurements from individual dislocation cells in deformed copper," (unpublished).
[15]Certain commercial equipment, instruments, or materials are identified in this paper to specify experimental or theoretical procedures. Such identification does not imply recommendation by NIST nor the authors, nor does it imply that the equipment or materials are necessarily the best available for the intended purpose.
[16]S. Olson and K. Hummler, "TSV reveal etch for 3D integration," in *Proceedings of the 3DIC, Osaka, Japan, Jan. 2012* (IEEE, 2012), pp. 1–4.
[17]A. S. Budiman *et al.*, "Measurement of stresses in Cu and Si around through-silicon via by synchrotron X-ray microdiffraction for 3-dimensional integrated circuits," Microelectron. Reliab. **52**, 530–533 (2012).
[18]H. Shin, B. Kim, J. Kim, S. Hwang, A. Budiman, H. Son, K. Byun, N. Tamura, M. Kunz, D. Kim, and Y. Joo, "Microstructure evolution and defect formation in Cu through-silicon vias (TSVs) during thermal annealing," J. Electron. Mater. **41**, 712–719 (2012).
[19]L. Lu, T. Zhu, Y. Shen, M. Dao, K. Lu, and S. Suresh, "Stress relaxation and the structure size-dependence of plastic deformation in nanotwinned copper," Acta Mater. **57**, 5165–5173 (2009).
[20]F. Dalla Torre, P. Spatig, R. Schaublin, and M. Victoria, "Deformation behaviour and microstructure of nanocrystalline electrodeposited and high pressure torsioned nickel," Acta Mater. **53**, 2337–2349 (2005).ôôôô
[21]Y. M. Wang and A. V. Hamza, "Activation volume and density of mobile dislocations in plastically deforming nanocrystalline Ni," Appl. Phys. Lett. **86**, 241917 (2005).
[22]S. Lagrange, S. H. Brongersma, M. Judelewicz, I. Vorvoort, E. Richard, R. Palmans, and K. Maex, "Self-annealing characterization of electroplated copper films," Microelectron. Eng. **50**, 449–457 (2000).
[23]K. B. Yin, Y. D. Xia, C. Y. Chan, W. Q. Zhang, Q. J. Wang, X. N. Zhao, A. D. Li, Z. G. Liu, M. W. Bayes, and K. W. Yee, "The kinetics and mechanism of room-temperature microstructural evolution in electroplated copper foils," Scr. Mater. **58**, 65–68 (2008).
[24]C. Okoro, K. Vanstreels, R. Labie, O. Lühn, B. Vandevelde, B. Verlinden, and D. Vandepitte, "Influence of annealing conditions on the mechanical and microstructural behavior of electroplated Cu-TSV," J. Micromech. Microeng. **20**, 045032 (2010).
[25]R. Rosenberg, D. C. Edelstein, C.-K. Hu, and K. P. Rodbell, "Copper metallization for high performance silicon technology," Annu. Rev. Mater. Sci. **30**, 229–262 (2000).

[26]J. Van Olmen, C. Huyghebaert, J. Coenen, J. Van Aelst, E. Sleeckx, A. Van Ammel, S. Armini, G. Kattiab, J. Vaes, W. Dehaene, E. Beyne, and Y. Travaly, "Integration challenges of copper Through Silicon Via (TSV) metallization for 3D-stacked IC integration," Microelectron. Eng. **88**, 745–748 (2011).
[27]I. De Wolf, K. Croes, O. Varela Pedreira, R. Labie, A. Redolfi, M. Van De Peer, K. Vanstreels, C. Okoro, B. Vandevelde, and E. Beyne, "Cu pumping in TSVs: Effect of pre-CMP thermal budget," Microelectron. Reliab. **51**, 1856–1859 (2011).
[28]J. Koike, S. Utsunomiya, Y. Shimoyama, K. Maruyama, and H. Oikawa, "Thermal cycling fatigue and deformation mechanism in aluminum alloy thin films on silicon," J. Mater. Res. **13**(11), 3256–3264 (1998).
[29]R. Schwaiger and O. Kraft, "High cycle fatigue of thin silver films investigated by dynamic microbeam deflection," Scr. Mater. **41**(8), 823–829 (1999).
[30]O. Kraft, R. Schwaiger, and P. Wellner, "Fatigue in thin films: Lifetime and damage formation," Mater. Sci. Eng., A **319–321**, 919–923 (2001).
[31]G. P. Zhang, C. A. Volkert, R. Schwaiger, R. Monig, and O. Kraft, "Fatigue and thermal fatigue damage analysis of thin metal films," Microelectron. Reliab. **47**, 2007–2013 (2007).
[32]Q. K. Zhang and Z. F. Zhang, "Thermal fatigue behaviors of Sn-4Ag/Cu solder joints at low strain amplitude," Mater. Sci. Eng. A **580**, 374–384 (2013).
[33]A. Mercha *et al.*, "Comprehensive analysis of the impact of single and arrays of through silicon vias induced stress on high-k/metal gate CMOS performances," in *International Electron Devices Meeting (IEDM), San Francisco, CA, Dec. 2010* (IEEE, 2010), pp. 2.2.1–2.2.4.
[34]W. Guo *et al.*, "Copper through silicon via induced keep out zone for 10nm node bulk FinFET CMOS technology," in *International Electron Devices Meeting (IEDM), Washington, DC, Dec. 2013* (IEEE, 2013), pp. 12.8.1–12.8.4.
[35]E. Beyne, "Electrical, thermal and mechanical impact of 3D TSV and 3D stacking technology on advanced CMOS devices—Technology directions," in 2011 IEEE International 3D Systems Integration Conference (3DIC), IEEE-CPMT, Osaka, Japan, 31 Jan.–2 Feb. 2012.